Available online at https://link.springer.com/journal/42241
http://www.jhydrodynamics.com
Journal of Hydrodynamics, 2021, 33(1): 104-110
https://doi.org/10.1007/s42241-021-0001-4

Experimental study of droplet behavior in a swirl flow field induced by two kinds of guiding vanes and inlet structure optimization *

Shi-ying Shi[1], Huan-qiang Sun[2], Li-ming Lin[1], Cheng-fu Zhang[3], Jian Zhang[1]
1. *Key Laboratory for Mechanics in Fluid Solid Systems, Institute of Mechanics, Chinese Academy of Sciences, Beijing 100190, China*
2. *Beijing-Hyundai Auto, Beijing 100190, China*
3. *Engineering Technology Branch, Cnooc Energy Development co., LTD, Tianjin 300452, China*

(Received June 6, 2020, Revised September 25, 2020, Accepted October 13, 2020, Published online February 4, 2021)

Abstract: Droplet breakage is a common phenomenon in converting a pipe flow to a swirl flow in a vane-type pipe separator (VTPS)' inlet. The evaluation of the dispersed droplet sizes after breakage is crucial to the optimum design of the inlet structure and the estimation of the oil-water separation performance. This paper studies the droplet behavior in a swirl flow produced by guiding vanes. Experiments are performed with two different guiding vanes at the inlet of the VTPS. The sizes of the produced oil droplets at the downstream of the guiding vanes are measured *in situ* using a Malvern Insitec SX. The results indicate that the streamlined deflector is superior to the semi-elliptical plate for the VTPS' optimization based on the comparison of the droplet sizes in their respective induced swirl flow fields, which can be explained by a modified T-model. Our study suggests that the use of the modified T-model is a reliable method to optimize the design of the guiding vane in the swirling generating stage.

Key words: Swirl flow field, droplet breakage mechanism, maximum droplet size, experiment

Introduction

The VTPS (Fig. 1) is a kind of highly efficient oil-water separator that utilizes the centrifugal forces produced by the different densities of the oil and the water to separate the oil and water phases in a high water-content mixture[1]. For a VTPS, the guiding vanes are the key to forming a swirling flow field and avoiding the extensive droplet breakage[2]. Therefore, the optimization of the guiding vanes is of great importance to the VTPS' efficiency and performance[3-4].

Despite the importance of the studies of the droplet produced in the swirl flow field for the oil-water separation, there is not much related experimental work being reported in the literature[5-7]. Oropeza-Vazquez[8] and Gomez[9] used the Rosin-Rammler droplet-size distribution expression, which was often adopted in the pipe flow, to predict the oil-water separation behavior in cyclones. In their model, the droplet-size distribution (DSD) is used as the basic information for establishing the separation calculation model. Schütz et al.[10] measured the DSDs in the cyclone feed flow, underflow and overflow with a laser spectroscope (Spraytec TM, Malvern TM). They found that the lower breakup rates could improve the separation behavior. However, they did not obtain the relationship between the cyclone's design parameters and the droplet size distribution in the swirl flow field during the breakage process. In 2013, Gao et al. [11] discovered that the breakup of the

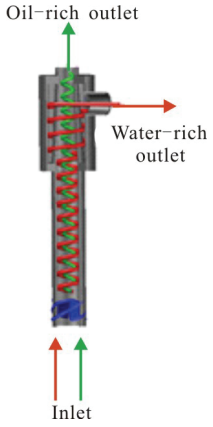

Fig. 1 (Color online) Schematic diagram of VTPS

* **Biography:** Shi-ying Shi (1984-), Female, Ph. D., Senior Engineering, E-mail: shishiying123@126.com
Corresponding author: Jian Zhang, E-mail: zhangjian20200925@163.com

oil droplets influences the oil-gas cyclone separator's separation efficiency.

In view of the studies reported in literature, this paper studies the droplet behavior in the swirl flow fields induced by two types of guiding vanes in the VTPS and thus optimizes the guiding vanes. The guiding vanes are evaluated by comparing the DSD produced by their respective swirling flow field. In view of the fact that no theoretical model is available for the prediction of the DSD in this pattern, experiments are performed for various oil contents and flow rates at the inlet of the vave-type pipe separator (VTPS). The cumulative volume fraction and the maximum droplet diameter of the dispersed phase are recorded using a laser particle size analyzer. Finally, the droplet size distributions are compared between these two types of guiding vanes to select a superior guiding vane for the oil-water separation. The droplet behavior is used to judge whether the guiding vanes are suitable for the high-efficient oil-water separation.

1. Droplet break-up theory

In order to describe the droplet behavior in a swirl flow, a distribution function is often needed. Karabelas[12] applied the Rosin-Rammler distribution function to describe the experimental data obtained from the pipe flows with a dispersed droplet distribution. However, the Rosin-Rammler distribution does not contain a mathematical upper cut-off, which is not practical in reality, especially when the droplets have a maximum drop diameter ($d_{\max}$) and will break in the turbulent flow above that size. Besides, the fit of this function with the oil droplet size distribution in a swirling flow field is not reliable.

1.1 *Hinze's (1955) model*

Currently, it is widely accepted that in the turbulent flow, the droplets can break by two types of stresses depending on the droplets size in relation with the smallest size of the possible eddies[13].

Hinze[14] argued that the drop breakup was mainly caused by its interaction with the turbulent eddies equal to or marginally smaller than the drop itself, since larger eddies simply transport the drop without breaking it while smaller ones lack sufficient energy to break the drop. In this instance, the maximum equilibrium droplet size of the dispersed phase is controlled by its mechanical stability against the dynamic pressure forces exerted by the turbulent motion of the surrounding continuous phase around it. When the internal viscous forces in the droplet are low enough to be neglected, Hinze's concept can be derived from the Young-Laplace equation as (H-model)

$$d_{\max} = 0.55D\left(\frac{\rho_c u_c^2 D}{\sigma}\right)^{-0.6} f^{-0.4} \tag{1}$$

where ρ_c is the density of the continuous phase, u_c is the velocity of the continuous phase, D is the hydraulic diameter, σ is the interfacial tension, $d_{\max}$ is the maximum stable dispersed phase droplet size and f is the friction factor[10-11].

$$f = \frac{0.046}{Re_c^{0.2}} = 0.046\left(\frac{\rho_c u_c D}{\eta_c}\right)^{-0.2} \tag{2}$$

where η_c is the dynamic viscosity of the water phase, Re is the Reynolds number.

The modified H-model is defined by Oropeza-Vazquez as follows[8]:

$$d_{\max} = 0.34\left(\frac{\sigma}{\rho_c}\right)^{0.6}\left(\frac{2f_1 u_c^3}{D}\right)^{-0.4} \tag{3}$$

$$f_1 = 0.046\left(\frac{\rho_c u_c D}{\mu_c}\right)^{-0.2} \tag{4}$$

where μ_c is the kinematic viscosity.

1.2 *Modified Tavlarides' model*

Coulaloglou and Tavlarides first proposed a series of phenomenological models to describe the drop breakup in the turbulently agitated liquid-liquid dispersions[15-18]. They suggested that a deformed drop will break once the turbulent kinetic energy was transmitted to the droplet by eddies exceeding its surface energy[19]:

$$\frac{\pi}{6}\rho_c d^3 \frac{\overline{u'^2}}{2} \geq \sigma\pi d^2 \tag{5}$$

$$We' = \frac{\rho_c \overline{u'^2} d}{\sigma} \geq 12 \tag{6}$$

where We' is the modified Weber number, d is the droplet diameter.

By applying this theory to the flow near the guide vane, the maximum drop diameter can be simplified as follows (Modified T-model)[17-18]

$$d_{\max} = \left(\frac{6\sigma}{\rho_c}\right)^{0.6}\left(\frac{V\rho_c}{Q_i \Delta p}\right)^{0.4} \tag{7}$$

where Q_i is the inlet flow rate, Δp is the pressure

drop loss across the guide vanes and V is the fluid volume across the guide vane.

2. Experiments

2.1 *Experimental setup*

To test the DSD in the swirling flow fields, an experimental system (Fig. 2) is established at the Laboratory of Applied Fluid Dynamics in Institute of Mechanics, Chinese Academy of Science. The experiments are conducted as follows: the oil and the water are pumped by separate pumps to a Y-junction to form a mixture. The mixture then flows through the guiding vanes in the VTPS. During the process, the oil droplets are broken into smaller ones and are detected by Malvern Insitec SX. After that, the mixture goes into a mixture tank and the different phases are separated finally. The separated oil is then pumped back to the oil tank while the remaining water flows out for an advanced treatment and is discharged. For the experiment, the LP-14 white oil and the deionized water are used as the experimental media. During the experiment, the temperature is controlled within a range of 16°C-18°C. Under these conditions, their densities and viscosities are as follows: $\rho_o = 836.0\ \mathrm{kg/m^3}$, $\mu_o \approx 0.215\ \mathrm{Pa \cdot s}$, $\mu_o \approx 0.215\ \mathrm{Pa \cdot s}$, $\rho_w = 998.2\ \mathrm{kg/m^3}$, $\mu_w \approx 0.001\ \mathrm{Pa \cdot s}$ and $\sigma = 0.045\ \mathrm{N/m}$.

2.2 *Guiding vanes*

In this experiment, the guiding vanes are installed in two concentric tubes of 0.025 m (in internal diameter, ID). The two types of guiding vanes are both made of transparent plexiglass (Figs. 3(a), 3(b)). Each guiding vane is at an angle of 30° to the cross section of the tube. The distance from the guiding vanes to the detection location is 0.2 m (Fig. 3(c)).

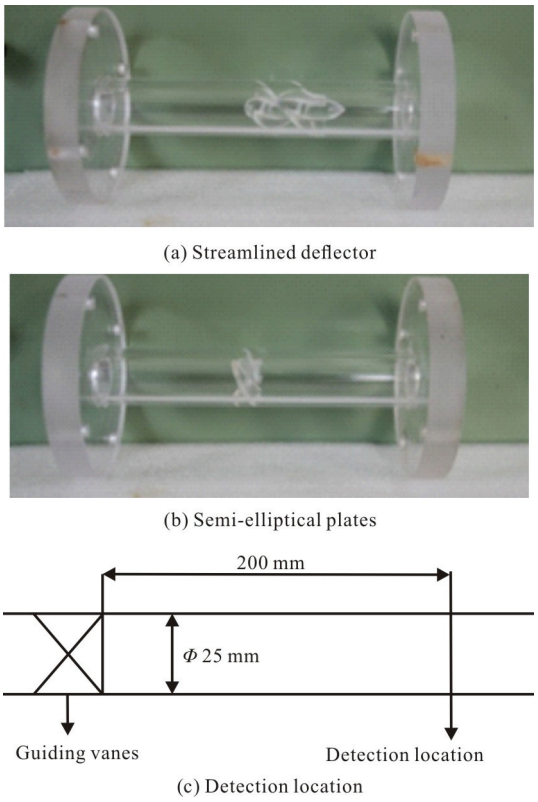

Fig. 3 (Color online) Photograph and schematic diagram for guiding vanes

2.3 *Measurement system*

We employ a laser spectroscope (Malvern Insitec SX) to measure the DSD in the swirling flow field right after the guiding vanes (Fig. 4). The working principle of the Malvern Insitec SX can be found in literature[20].

3. Results and discussions

In this section, the experiment results will be

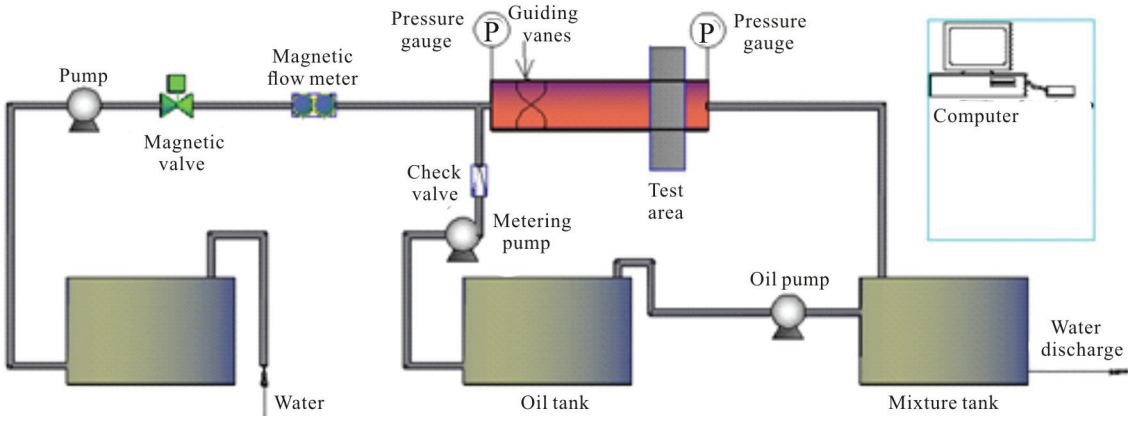

Fig. 2 (Color online) Experimental system for measuring DSD after guiding vanes

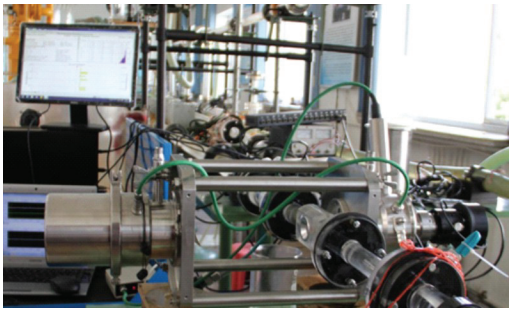

Fig. 4 (Color online) Diagram of the Malvern Insitec SX in the pipe

discussed, and the guiding vanes are optimized for the VTPS to work more efficiently.

3.1 *The effect of water content on DSD*

The results in Fig. 5 show the effect of the water content on the DSD at a mixture velocity of 1.87 m/s in a swirl flow induced by the guiding vanes. It can be observed that as the water content decreases, the peak value of the DSD moves towards the right side and the volume fraction of the larger droplets begins to increase. In other words, it seems that the DSD changes from an unimodal distribution to a bimodal distribution for larger droplets'size that exceeds the scope of the instrument. When the water content is more than 99%, the DSD is in a clear distribution pattern. Hence, a dilute dispersion (with the water content more than 99%) mixture is used for subsequent experiments in this paper. Both type of guiding vanes are observed to obey the same law. Furthermore, it can be observed that the droplet size corresponding to the peak value for the streamlined deflector is larger than that for the semi-elliptical under the same conditions. This may be explained by the fact that the oil droplets break more thoroughly when crossing the semi-elliptical plates.

3.2 *The effect of the inlet water velocity*

Figure 6(a) shows the changes of the DSD induced by two kinds of guiding vanes when the inlet water velocity increases in the dilute dispersion. It can be observed that as the velocities increase, the peak values of the DSD decrease under the different conditions. This is a common phenomenon as a higher speed results in a larger shear force on the oil droplet. Moreover, at the same inlet water velocities, the DSD in the VTPS with the semi-elliptical plates is located relatively on the left to that of the streamlined deflector. This indicates that fewer oil droplets break when they flow through the streamlined deflector. When the

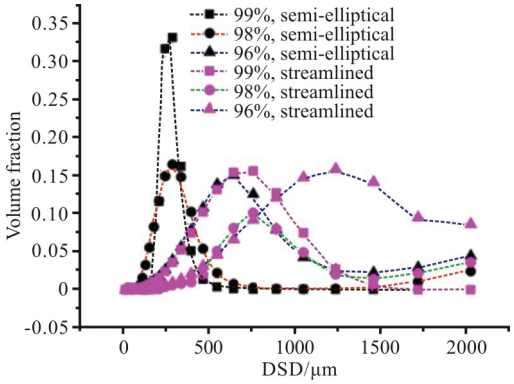

Fig. 5 (Color online) DSD of different oil contents at same inlet flow rate velocity of 1.87 m/s

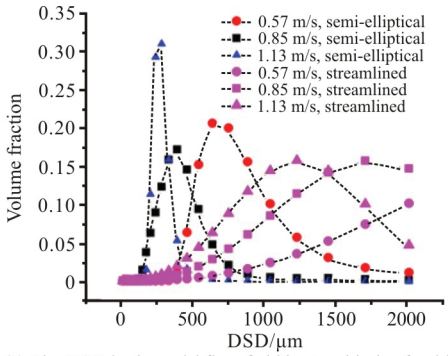

(a) The DSD in the swirl flow field by two kinds of guiding vanes

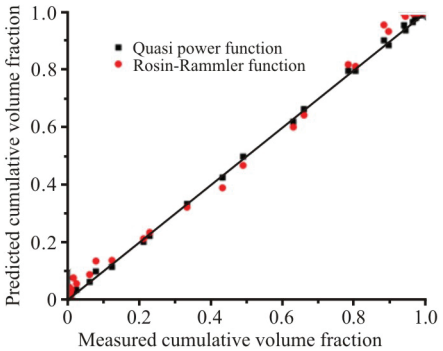

(b) Comparing between experiments and different functions

Fig. 6 (Color online) The influence of inlet water velocity on droplet size distribution

velocity at the inlet is less than 1.13 m/s, the DSD in the VTPS with the streamlined deflector is beyond the measuring range of the instrument.

The Rosin-Rammler function is often used to describe the cumulative volume fraction distribution for the oil-water two phase pipe flows[8]. The DSD in a swirl flow field is changed by the guiding vanes when the mixture flows through it. So a kind of quasi-power function is used to fit the DSD in the swirl flow field generated by the guiding vanes. Figure 6(b) compares the two kinds of functions with

the experimental results. It can be seen that the quasi power function defined by the following equation fits the experiments better than the Rosin-Rammler function. This can be easily explained. Before the guiding vanes, the DSD always could be described by the Rosin-Rammler function. But when the oil droplets flow through the guiding vanes, not all droplets will breakup into small ones. So the DSD in a swirl flow field changes.

$$F(d)=\frac{1}{1+(d/a)^b} \tag{8}$$

where a and d are parameters.

3.3 *The effect of the inlet water velocity on the maximum droplet size*

The maximum stable droplet size is the key to determine the overall location of the DSD. The larger the maximum stable droplet size, the closer the DSD is to the large oil droplet indicating a larger average droplet size (Fig. 6(a)). Therefore, it is necessary to study the variation of the maximum stable droplet size. Figure 7 shows the maximum droplet size at different inlet water velocities for droplets in the VTPS with the semi-elliptical plates in dilute dispersions ($\leq 1\%$). The results in Fig. 7(a) show that as the inlet water velocity increases, the maximum droplet diameter decreases. This may be explained by the fact that the shear stress imposed on the droplets by the continuous phase increases with the increase of the inlet velocity. Additionally, the pressure drop loss, which is shown in Fig. 7(b), increases also with the increase of the inlet velocity.

The high pressure drop loss indicates that the internal friction loss is large. As a result, the droplets become increasingly likely to break into smaller ones. That can be explained by the breakage mechanism of the oil droplets while passing through the guide vane.

3.4 *Criterion for choosing the optimal guiding vanes for the VTPS*

From the analysis of the experimental data, one can conclude that the larger the maximum droplet size, the larger the average droplet size, which is beneficial in improving the separation efficiency of the VTPS. Therefore, the maximum stable droplet size in an induced swirl flow field is used as the criterion for choosing the optimal guiding vanes.

To calculate the maximum droplet size using theoretical models, the pressure drop across the guiding vanes is detected by two pressure transducers. As the pipe is placed horizontally with the two pressure transducers also installed at the same height, without the gravitational effect on the pressure drop. Furthermore, the pipe between the pressure sensors is a straight pipe with a constant diameter. Hence, the pressure drop and the mean rate of the energy dissipation, $\bar{e}$, can be calculated precisely without external interferences.

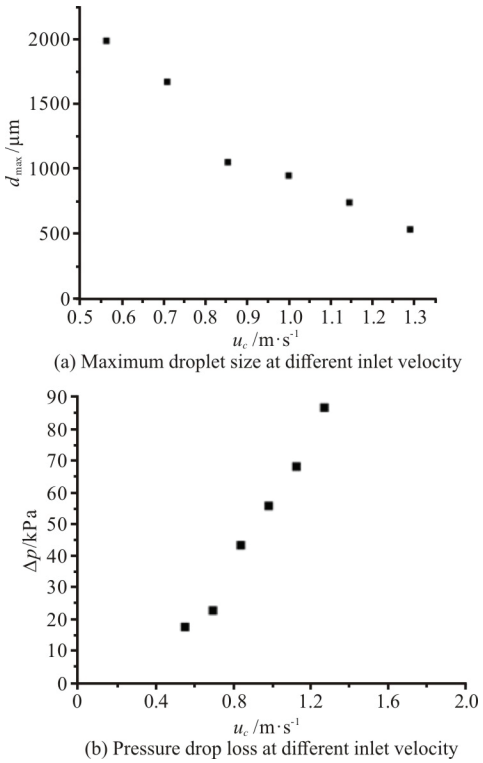

Fig. 7 Experimental results of the flow through semi-elliptical plates in a swirl flow at different inlet water velocities

Figures 8(a), 8(b) show comparisons of the droplet size in the dilute dispersions observed experimentally with the expected sizes deduced by calculations based on the H-model, the modified H-model and the modified T-model. Evidently, that maximum droplet size is overestimated and underestimated by the H-model and the modified H-model, respectively, as compared to the experiments, because these two models were actually developed for the droplet breakage in a turbulent pipe flow. In a swirl flow field, the model to calculate the mean energy dissipation in the generation stage of a swirl flow needs to consider not only the friction pressure drop between the continuous phase and the wall of the pipe, but also the energy loss during the swirling flow generation such as the droplet breakage. From the aforementioned comparison, a conclusion can be made that the droplet breaks if the kinetic energy of the turbulent motion exceeds the free surface energy of the droplet. If the modified Weber number We' is larger than 12, the large droplet will break up into smaller ones.

As discussed previously, it can be seen that the modified T-model is more suitable to explain the mechanism of the droplet breakage in the swirl flow

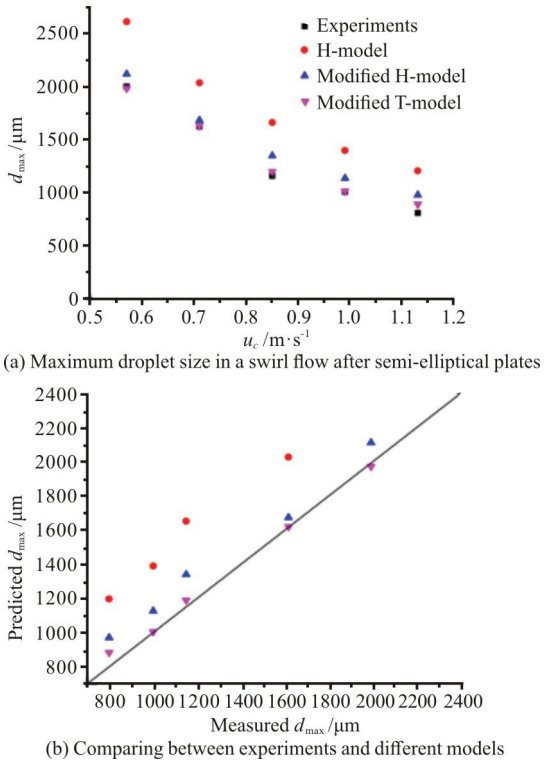

(a) Maximum droplet size in a swirl flow after semi-elliptical plates

(b) Comparing between experiments and different models

Fig. 8 (Color online) Comparison of measured values of d_{max} in the swirl flow field generated by the semi-elliptical plates with different models in dilute dispersions

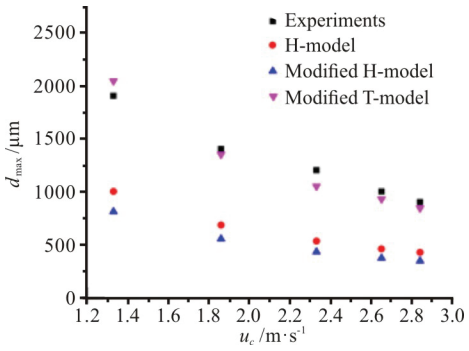

Fig. 9 (Color online) Comparison of measured values of d_{max} in the swirl flow field generated by the streamlined deflector with different models in dilute dispersions

field generated by the semi-elliptical plates. From Eq. (7) we can conclude that when the properties of the fluid are fixed, the smaller the pressure drop across the guiding vanes, the larger the maximum droplet size. To verify this conclusion, further experiments are conducted to study the swirl flow field generated by the streamlined deflector. The maximum droplet is measured and the results are shown in Fig. 9. By comparing Figs. 8(a), 9, it is observed that the maximum droplet size is larger in the swirl flow field generated by the streamlined deflector under the same conditions. Hence, the larger the droplet is, the higher the oil-water separation efficiency is in the swirl flow field.

3.5 *The optimized guiding vanes for oil-water separation*

As the swirling flow field generated by the streamlined deflector produces a larger maximum stable droplet size, theoretically speaking, it has a higher oil-water separation efficiency. To verify this viewpoint, experiments are carried out to see whether the oil core agglomerates better by using the streamlined deflector.

Figure 10 shows the effect of the droplet size on the oil-water separation performance at an inlet velocity speed of 1.7 m/s and an inlet oil content of 0.06. The results indicate that the average droplet in the swirl flow field induced by the streamlined deflector is larger than that induced by the semi-elliptical plates. When the inlet oil flow rate is kept the same, the average droplet size becomes larger with the decrease of the droplet number. Therefore, the formation of the oil cores is much faster in the swirl field induced by the streamlined deflector, which is favorable to the separation. The experimental results show that our optimization for the guiding vanes is effective.

4. Conclusions

In this paper, the characteristics of the DSD, the maximum droplet size and the cumulative volume fraction in a swirl flow field induced by two different kinds of guiding vanes in the VTPS are experimentally studied using a Malvern particle size analyzer. From the droplet behavior in the swirling flow field, the following conclusions can be drawn.

As the water content increases, the peak of the DSD moves towards the droplet of smaller diameter and the pattern of the DSD changes from unimodal to bimodal distributions. The droplet size corresponding to the peak value for the streamlined deflector is larger than that for the semi-elliptical deflector under the same conditions. Besides, a quasi-power function can be used to describe the DSD in the swirl flow field generated by the guiding vanes.

When the inlet water velocity increases, the oil droplet size corresponding to the peak value of the DSD curve decreases. As compared with other deflectors, the oil droplets break less when they flow through the streamlined deflector, implying that the streamlined deflector does better in improving the performance of the VTPS.

The maximum droplet sizes in a swirl flow field induced by guiding vanes may be described precisely by the modified T-model. The droplet breaks up as the kinetic energy of the turbulent motion exceeds the free

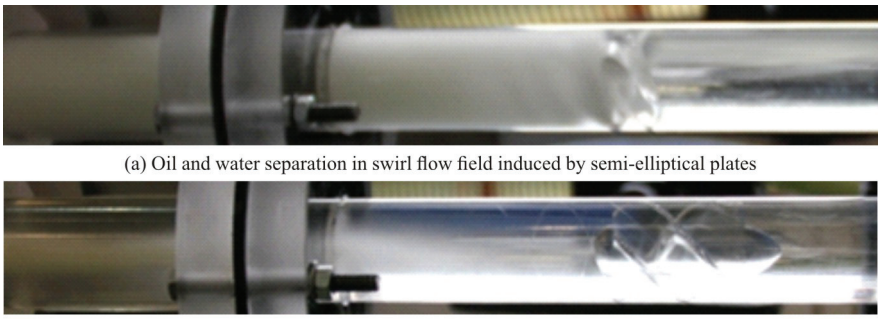

(a) Oil and water separation in swirl flow field induced by semi-elliptical plates

(b) Oil and water separation in swirl flow field induced by streamlined deflector

Fig. 10 (Color online) Comparison of oil-water separation in swirl flow field

surface energy of the droplet. When the modified Weber number We' is larger than 12, the droplet becomes easy to break up into smaller ones. As the fluid flows through the guiding vanes, the energy loss is reduced, which can significantly reduce the probability of the droplet breakage. This law can also be used in the inlet structure optimization of other types of separators.

This study provides a theoretical basis for the optimization and the industrial application of the VTPS.

References

[1] Shi S. Y., Xu J. Y., Sun H. Q. et al. Experimental study of a vane-type pipe separator for oil–water separation [J]. *Chemical Engineering Research and Design*, 2012, 90(10): 1652-1659.

[2] Deng Y., Yu B., Sun D. Multi-objective optimization of guide vanes for axial flow cyclone using CFD, SVM, and NSGA Ⅱ algorithm [J]. *Powder Technology*, 2020, 373: 637-646.

[3] Liu M. L., Chen J. Q., Cai X. L. et al. Oil-water pre-separation with a novel axial hydrocyclone [J]. *Chinese Journal of Chemical Engineering*, 2018, 26(1): 60-66.

[4] Sailesh C., Hari P. N., Ole G. Development of a test rig for investigating the flow field around guide vanes of Francis turbines [J]. *Flow Measurement and Instrumentation*, 2019, 70: 101648.

[5] Tian J., Ni L., Song T. et al. An overview of operating parameters and conditions in hydrocyclones for enhanced separations [J]. *Separation and Purification Technology*, 2018, 206: 268-285.

[6] Gayatree P., Bhargava V., Meikap B. C. Performance evaluation of a hydrocyclone with a spiral rib for separation of particles [J]. *Advanced Powder Technology*, 2017, 28(12): 3222-3232.

[7] Banerjee C., Climent E., Majumder A. K. Mechanistic modelling of water partitioning behavior in hydrocyclone [J]. *Chemical Engineering Science*, 2016, 152: 724-735.

[8] Oropeza-Vazquez C., Afanador E., Gomez L. et al. Oil-water separation in a novel liquid-liquid cylindrical cyclone (LLCC©) compact separator–Experiments and modeling [J]. *Journal of Fluids Engineering*, 2004, 126(4): 1657-1671.

[9] Carlos G., Juan C., Wang S. et al. Oil-water separation in liquid-liquid hydrycyclones (LLHC)-experiment and modeling [C]. *SPE Annual Technical Conference and Exhibition*, New Orleans, Louisiana, 2001, 1-18.

[10] Schütz S., Gorbach G., Piesche M. Modeling fluid behavior and droplet interactions during liquid–liquid separation in hydrocyclones [J]. *Chemical Engineering Science*, 2009, 64(18): 3935-3952.

[11] Gao X., Chen J., Feng J. et al. Numerical and experimental investigations of the effects of the breakup of oil droplets on the performance of oil-gas cyclone separators in oil-injected compressor systems [J]. *International Journal of Refrigeration*, 2013, 36(7): 1894-1904.

[12] Karabelas A. J. Droplet size spectra generated in turbulent pipe flow of dilute liquid/liquid dispersions [J]. *AIChE Journal*, 1978, 24(2): 170-180.

[13] Hert S. C. D., Rodgers T. L. On the effect of dispersed phase viscosity and mean residence time on the droplet size distribution for high-shear mixers [J]. *Chemical Engineering Science*, 2017, 172: 423-433.

[14] Hinze J. O. Fundamentals of the hydrodynamic mechanism of splitting in dispersion processes [J]. *AIChE Journal*, 1955, 1(3): 289-295.

[15] Coulaloglou C. A., Tavlarides L. L. Description of interaction processes in agitated liquid-liquid dispersions [J]. *Chemical Engineering Science*, 1977, 32(11): 1289-1297.

[16] Bai J. X., Huang Y. X., Jiang N. et al. Experimental investigation on wall-bounded turbulence drag reduction by double piezoelectric vibrator active control [J]. *Journal of Hydrodynamic*s, 2020, 32(5): 747-757.

[17] Batchelor G. K. Pressure fluctuations in isotropic turbulence [J]. *Mathematical Proceedings of the Cambridge Philosophical Society*, 1951, 47(2): 359-374.

[18] Zhang A. M., Sun P. N., Ming F. R. et al. Smoothed particle hydrodynamics and its applications in fluid-structure interactions [J]. *Journal of Hydrodynamics,* 2017, 29(2): 187-216.

[19] Listewnik J. Some factors influencing the performance of de-oiling hydrocyclones for marine application [C]. *Proceedins of the 2nd International Conference on Hydrocyclone*, Bath, England, UK, 1984, 191-204.

[20] Shi S. Y., Liang C. C., Zhang D. et al. Investigation of oil droplet distribution in a vane-type pipe separator [J]. *International conference on Applied Mechanics and Mechanical Automation (AMMA)*, Hong Kong, China, 2017.